



Compression behaviour of anhydrous and hydrate forms of sodium naproxen

Ledjan Malaj^a, Roberta Censi^{b,c}, Zehadin Gashi^a, Piera Di Martino^{c,*}

^a Department of Pharmacy, University of Tirana, Albania

^b Utrecht Institute of Pharmaceutical Sciences (UIPS), University of Utrecht, The Netherlands

^c Department of Chemical Sciences, University of Camerino, Via S. Agostino, 1, 62032 Camerino, Italy

ARTICLE INFO

Article history:

Received 13 October 2009

Received in revised form 15 January 2010

Accepted 23 January 2010

Available online 1 February 2010

Keywords:

Sodium naproxen

Hydrates

Tableting

Densification

ABSTRACT

The aim of the present work was to investigate the technological properties and the compression behaviour of the anhydrous and hydrate solid forms of sodium naproxen. Among the hydrates, the following forms were studied: the monohydrate (MSN), obtained by dehydrating a dihydrated form (DSN) in each turn obtained by exposing the anhydrous form at 55% RH; a dihydrated form (CSN) obtained by crystallizing sodium naproxen from water, the tetrahydrated form (TSN) obtained by exposing the anhydrous form at 75% RH. The physico-chemical (crystalline form and water content), the micromeritic (crystal morphology and particle size) and the mechanical properties (Carr's index, apparent particle density, compression behaviour, elastic recovery and strength of compact) were evaluated.

We made every effort to reduce differences in crystal habit, particle size and distribution, and amount of absorbed water among the samples, so that the only factors affecting their technological behaviour would be the degree of hydration and the crystalline structure. This study demonstrates a correlation between the compression behaviour and the water molecules present in the crystalline structures. The sites where water molecules are accommodated in the crystalline structure behave like weak points where the crystalline lattice yields under compression. The crystal deformability is proportional to the number of water molecules in these sites; the higher the water content, the higher the deformability, because the densification behaviour changes from a predominantly elastic deformation to a plastic behaviour. The deformability is responsible for a higher densification tendency that favours larger interparticle bonding areas that may explain the better tableability of TSN and CSN.

© 2010 Elsevier B.V. All rights reserved.

1. Introduction

In a previous paper (Di Martino et al., 2008), the authors demonstrated that when subjected to wet granulation in a high-shear mixer–granulator, the anhydrous form of sodium naproxen (ASN) undergoes hydration to the tetrahydrated form. Subsequent drying can lead to granules with varying degrees of hydration, which has important repercussions on their performance under compression. Observing that granule tableability increased with degree of hydration, the authors supposed that the phenomenon could be related either to differences in the crystalline form of sodium naproxen or to differences in water content.

In a subsequent paper (Joiris et al., 2008), the same authors observed the hydration of anhydrous sodium naproxen (ASN) exposed at two different RH% and concluded that hydration considerably affects sodium naproxen's compression behaviour; in general, the higher the water content, the higher the tableability. These results were directly related to an increase in plastic deformation accompanied by a decrease in elastic recovery.

Compression behaviour results were analysed together with the hydration process, and it was concluded that during hydration, water molecules enter the crystal along hydrophilic tunnels, perturbing the crystallographic structure and causing slight structural changes, according to the amount of water. The interposition of water molecules between sodium naproxen molecules weakens intermolecular bonds, and these sites can behave like sliding planes under compression. This conclusion was in agreement with the studies of Sun and Grant (2004), who explained that the greater tableability of the monohydrated form of *p*-hydroxybenzoic acid compared to the anhydrous one was due to the presence of water between molecule planes. In fact, the water molecules fill the spaces between the layers, increasing the interparticle bonding area and facilitating crystal plastic deformation.

The aim of the present work was to characterize the compression behaviour of different pure forms of sodium naproxen, by taking into account the role played by the water included in the crystals. The following properties were considered: the physico-chemical (crystalline form and water content), the micromeritic (crystal morphology and particle size) and the mechanical ones (Carr's index, apparent particle density, compression behaviour,

* Corresponding author. Tel.: +39 0737 402215; fax: +39 0737 637345.
E-mail address: piera.dimartino@unicam.it (P. Di Martino).

elastic recovery and strength of compact). The following crystalline forms were considered:

- (a) anhydrous sodium naproxen (ASN);
- (b) monohydrated sodium naproxen (MSN), obtained by dehydrating dihydrated sodium naproxen (DSN), according to Kim and Rousseau (2004);
- (c) a dihydrated sodium naproxen (DSN), obtained by exposing the ASN at 55% RH according to Di Martino et al. (2001);
- (d) a dihydrated sodium naproxen (CSN), obtained by crystallizing sodium naproxen from water, according to Di Martino et al. (2001) and Kim and Rousseau (2004);
- (e) the tetrahydrated form (TSN), obtained by exposing the ASN at 75% RH according to Di Martino et al. (2007).

Compared to the previous work (Joiris et al., 2008), in which the compression behaviour and the evolution of the densification mechanism were evaluated as the hydration of anhydrous sodium naproxen proceeded, this study devoted greater attention to the technological properties of the final hydrates. In particular, the authors wanted to elucidate the effect of water inclusion in the crystal lattice, as well as the effect of crystalline structure on the compression behaviour of sodium naproxen.

During this study, particular emphasis was given to the differences between CSN and the DSN, because they possess the same amount of bound water, but have different crystalline forms (Malaj et al., 2009).

2. Experimental

2.1. Materials

Anhydrous sodium naproxen (ASN) B.P. was kindly supplied by ACRAF (Ancona, Italy). During the present study, four different hydrated forms of sodium naproxen were used:

- (a) the monohydrate form (MSN) was obtained by dehydrating DSN under desiccation, according to Kim and Rousseau (2004); dehydration was followed by X-ray powder diffractometry and thermogravimetry and stopped when the desired structure was obtained;
- (b) one dihydrate form (CSN) was recovered by crystallizing ASN from water (Di Martino et al., 2001);
- (c) a second dihydrate form (DSN) was obtained by exposing the ASN at a relative humidity of $55 \pm 2\%$, according to the method described by Di Martino et al. (2001);
- (d) the tetrahydrated form (TSN) was obtained by exposing the ASN at a RH of $75 \pm 2\%$ (Di Martino et al., 2007).

The procedure for the hydration of the last two forms, extensively described in a previous paper (Joiris et al., 2008), is based on the general description of Kontny and Zografi (1995). Briefly, powder hydration was carried out by storing powders in an incubator (Velp Scientifica, FTC 90E, Usmate, Italy) at 25°C under the two different RH values of 55% and 75%. The RH was checked by a thermohygrometer (Universal Enterprise Inc., Cambiago, Milano, Italy), and their hydration was followed by X-ray powder diffractometry and thermogravimetry. To generate controlled relative humidity levels of $55 \pm 2\%$ and $75 \pm 2\%$, two different salts were used, Mg nitrate and Na chloride, respectively (Sigma Aldrich, Stenheim, Germany).

All the powders were sieved in order to collect the same granulometric fraction of 0–100 μm .

2.2. Physico-chemical characterization

The crystalline form of hydrated forms was checked by X-ray powder diffractometry (XRPD), using a Philips PW 1730 (Philips Electronic Instruments Corp., Mahwah, NJ, USA) as X-ray generator for Cu K α radiation ($\lambda_{\alpha 1} = 1.54056 \text{ \AA}$, $\lambda_{\alpha 2} = 1.54430 \text{ \AA}$). The experimental X-ray powder patterns were recorded on a Philips PH 8203 apparatus. The goniometer supply was a Philips PW 1373 and the channel control was a Philips PW 1390. Data were collected in the discontinuous scan mode using a step size of $0.01^\circ 2\theta$. The scanned range was $2\text{--}40^\circ (2\theta)$.

The total water content of the samples after equilibration was determined by simultaneous thermal analysis (STA), which can simultaneously analyse a sample for change in weight (thermogravimetric analysis, TGA) and change in enthalpy flow (differential scanning calorimetry, DSC). The analysis was performed with a simultaneous thermal analyser (STA 6000, Perkin Elmer, Inc., Waltham, MA, USA), under nitrogen atmosphere (20 ml/min) in 0.07 ml open aluminium oxide pans. STA was calibrated for temperature and heat flow with three standard metals (tin, indium and zinc), taking into account their expected melting temperatures (505.08, 429.75 and 692.68 K respectively), and for weight with an external Perkin Elmer standard (Calibration Reference Weight P/N N520-0042, Material lot 91101 GB, Weight 55.98 mg, 01/23/08 VT). Calibration was repeatedly checked to assure deviation $\leq \pm 0.3 \text{ K}$. The scanning analysis was performed on samples (approximately 10 mg) tested in quadruplicate by heating them from 293 to 533 K at a heating rate of 10 K min^{-1} .

2.3. Determination of micromeritic and mechanical properties

Crystal morphology was characterized using a scanning electron microscope (SEM) (Stereoscan 360, Cambridge Instruments, Cambridge, United Kingdom). Samples were mounted on a metal stub with double-sided adhesive tape and then sputtered under vacuum with a gold layer of about 200 \AA thickness using a metalizer (Balzer MED 010, Linchestein). Particle size was determined by counting the Ferret's diameter of 500 particles.

Carr's index (1965a,b) was determined from powder volumes at the initial stage and at constant volume (Tecnogalenica, Italy).

Apparent particle densities of native crystals, necessary to determine the tablet porosity during compression and densification, were measured using a helium pycnometer (Accupyc 1330, Micromeritics, England) with a cell of 10 cm^3 . Results are the mean of 10 measurements.

Compression was carried out in an instrumented single punch tablet machine (Frogerais OA, Vitry, France), equipped with flat punches of 11.28 mm in diameter. Five cycles were performed for every substance, reaching a maximum punch pressure of about 150 MPa. The die depth was fixed at 10.00 mm. External lubrication was obtained by compressing microcrystalline cellulose along with 1% (w/w) magnesium stearate. For each tablet, an appropriate amount of powder was weighed and introduced manually into the die. The machine was started and measures were recorded at a frequency of 2000 Hz. The length of pressure application on the powder (compression and decompression) was about 150 ms. Correction of displacement transducer data for machine looseness and punch deformation was carried out according to Juslin and Paronen (1980). Pressure transmission through the powder bed in the die was estimated by comparing maximum compression pressures on the upper and lower punches. The transmission coefficient corresponds to the ratio of lower punch and upper punch values. Once recovered, mass, thickness and crushing strength of tablets were measured, with a scale (Precisa XT220 A), a micrometer (Mitutoyo, Japan) and a strength tester (Tablet Tester 8 M, Schleuniger, Switzerland) respectively. Tensile strength Q (Fell and Newton,

1970) was calculated according to Eq. (1):

$$Q = \frac{2H}{\pi dt} \quad (1)$$

where H is the tablet crushing strength, d the diameter and t the thickness.

The densification behaviour of powders was studied using Heckel's equation (1961):

$$\ln \frac{1}{1-D} = KP + A \quad (2)$$

where D is the relative density of the compressed powder bed at applied pressure P . K is the slope of the straight linear portion of Heckel's plot and the reciprocal of K is the mean yield pressure (P_Y). The constant A is the sum of two densification terms:

$$A = \ln \left(\frac{1}{1-D'_0} \right) + B \quad (3)$$

According to Doelker (1994), D'_0 corresponds to the relative density of the powder at the moment when the last recorded applied pressure is still nil, and B is the densification due to particle fragmentation. Constants A and B can be expressed as relative densities using:

$$D_A = 1 - e^{-A} \quad (4)$$

$$D'_B = D_A - D'_0 \quad (5)$$

Heckel's profiles were established from single compression cycles on tablets compressed approximately at 150 MPa. Parameters P_Y , D_A , D'_0 , D'_B were calculated using a pre-compression pressure value of 2.0 MPa. Several methods have been described to select a linear region of the Heckel function in order to determine Heckel constants. Following Paronen and Ilkka (1996), we selected a range of measurement points where the linear regression coefficient was as high as possible. This corresponded to the 50–100 MPa range for both samples, with coefficient values superior to 0.998. Each value was a mean of five measurements.

Total elastic recovery (TER) was calculated according to Armstrong and Haines-Nutt (1974):

$$\text{TER} = \frac{t_2 - t_1}{t_1} \times 100 \quad (6)$$

where t_1 is the minimal thickness of the powder bed in the die and t_2 is tablet thickness.

3. Results

3.1. Physico-chemical characterization

All the powders were first analyzed by XRPD to check their crystalline form, comparing their powder patterns with those of known forms. The analysis confirmed the compliance of all the powders with the crystalline forms previously characterized. In particular, the patterns of ASN and CSN complied with Kim and Rousseau (2004) and Di Martino et al. (2007), those of MSN complied with Kim and Rousseau (2004), and those of DSN and TSN complied with Di Martino et al. (2007). It is important to note that the two hydrated forms, DSN and CSN, had different crystalline forms, even though they have similar water content, as already demonstrated in a previous work (Malaj et al., 2009).

The interaction of water with pharmaceutical powders is one of the most important factors affecting their tableting performance (Khankari and Grant, 1995).

Water can be present in powders in different physical forms: as adsorbed monolayers or multilayers on the surfaces of the particles, as condensed water on the surface, as physically absorbed water within the particles, or as strongly bound water (Malamataris

Table 1

Formula and water content for the sodium naproxen forms.

| Form | Formula | Molecular weight (Da) | Total water content (%) ^a | Theoretical water content (%) |
|------|---|-----------------------|--------------------------------------|-------------------------------|
| ASN | C ₁₄ H ₁₃ O ₃ Na | 252 | 0.07 ± 0.03 | 0.0 |
| MSN | C ₁₄ H ₁₃ O ₃ Na·H ₂ O | 270 | 6.68 ± 1.03 | 6.66 |
| CSN | C ₁₄ H ₁₃ O ₃ Na·2H ₂ O | 288 | 12.95 ± 1.15 | 12.49 |
| DSN | C ₁₄ H ₁₃ O ₃ Na·2H ₂ O | 288 | 12.86 ± 2.78 | 12.49 |
| TSN | C ₁₄ H ₁₃ O ₃ Na·4H ₂ O | 324 | 21.79 ± 2.24 | 22.22 |

^a Determined by simultaneous thermal analysis (TGA–STA).

et al., 1991). The objective of this study was to evaluate how the water bound in the SN crystalline structure influences compression behaviour, separately from the effect exhibited by the water absorbed on the particle surface. To this end, 0–100 μm fractions of all samples were stored as a thin layer on an aluminium plate for 2 h under vacuum and at 25 ± 2 °C in order to reduce the difference in surface moisture between the samples (Sun and Grant, 2004). As proven by X-ray powder diffractometry, the powders are stable in these conditions and this treatment limited the possible effect of absorbed water. The fact that there were only negligible differences in the amount of absorbed water among the samples is clearly evident in the results of Table 1, where the total water content determined by TGA–STA is given together with the theoretical water content. While the water content was always in compliance with the theoretical one, it was always slightly higher than expected (max 3.55%), thus it is possible that the excess water was absorbed on the particle surface. This rough approximation was necessary because desolvation of hydrated forms of SN already occurs at temperatures near to room temperatures (Di Martino et al., 2001; Kim and Rousseau, 2004), so it is difficult to accurately determine the amount of water that is part of the crystalline structure of SN (bound water) and the amount simply absorbed into the crystal surface (unbound water) by any thermogravimetric methods.

3.2. Determination of micromeritic properties

As mentioned above, for the purposes of this study it was important to level off all the parameters that might affect compression behaviour, the better to evaluate crystalline form and the degree of hydration as unique variables among the samples. Thus the same granulometric fraction was chosen for all the samples, as described in Section 2.1. In addition, most of the samples were prepared from ASN by a hydration (DSN, TSN) or dehydration (MSN) process, and as already proven in a previous study (Joiris et al., 2008), the hydration of original ASN particles affects neither particle size nor particle shape. Fig. 1 shows SEM micrographs of SN samples at constant resolution; it can be seen that not even the differences between the CSN (produced by crystallization from water) and the other samples were significant. In general, particles of all the samples appeared as irregular crystals composed of large particles with quite rounded and smoothed edges in the presence of irregular and smaller particles.

The similarity in particle morphology affects granulometric particle distribution. As demonstrated in Fig. 2, the particle size distribution was very similar for all the samples and non-statistically relevant differences could be observed (the statistical significance was evaluated by a one-way ANOVA test for $\alpha = 0.05$).

Other micromeritic properties are given in Table 2. The apparent particle densities were measured to evaluate powder densification using Heckel's equation. Apparent particle densities decreased in the order ASN > CSN > MSN > DSN > TSN, therefore, in general, they decreased with the increase in degree of hydration. The only exception occurred with CSN. As will be shown below, CSN behaviour

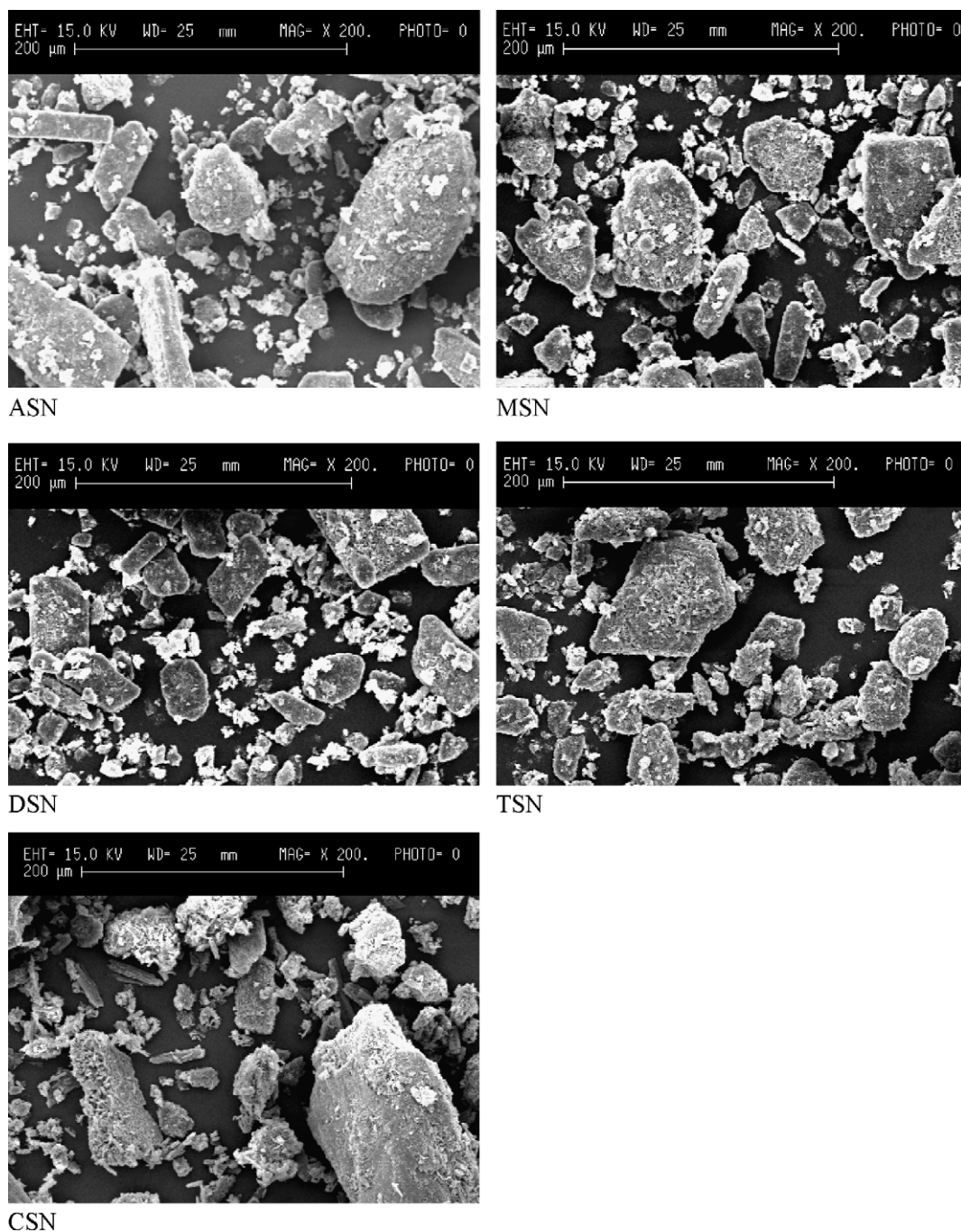


Fig. 1. SEM microphotographs (200 \times) of SN crystals. (a) ASN; (b) MSN; (c) DSN (55%RH); (d) TSN (76%RH); (e) CSN.

Table 2

Micromeritic properties and results of compactibility study of sodium naproxen anhydrous and hydrated forms.

| | ASN | MSN | CSN | DSN | TSN |
|---|-------------------|-------------------|-------------------|-------------------|-------------------|
| Apparent particle density (g cm^{-3}) ^a | 1.374 ± 0.001 | 1.352 ± 0.002 | 1.360 ± 0.003 | 1.341 ± 0.001 | 1.333 ± 0.001 |
| Bulk density (g cm^{-3}) ^b | 0.506 ± 0.004 | 0.523 ± 0.005 | 0.500 ± 0.024 | 0.554 ± 0.002 | 0.570 ± 0.003 |
| Tapped density (g cm^{-3}) ^c | 0.639 ± 0.002 | 0.651 ± 0.013 | 0.619 ± 0.027 | 0.662 ± 0.017 | 0.673 ± 0.015 |
| Carr's index ^d | 20.94 | 18.29 | 19.97 | 16.27 | 15.30 |
| σ_0 (MPa) ^e | 2.05 ± 0.02 | 2.88 ± 0.03 | 3.50 ± 0.02 | 2.99 ± 0.01 | 3.47 ± 0.02 |
| R^f | -0.98 | -0.99 | -0.99 | -0.98 | -0.99 |

^a Determined by helium pycnometry. Standard deviations are also indicated.

^b Determined from the volume of 100 g of powder. Standard deviations are also indicated.

^c Determined from the volume of 100 g of powder after 500 tapping to constant volume. Standard deviations are also indicated.

^d Calculated from bulk and tapped densities.

^e Tablet tensile strength extrapolated to zero porosity in Eq. (7). The 95% confidence intervals are indicated.

^f Linear regression of Eq. (7).

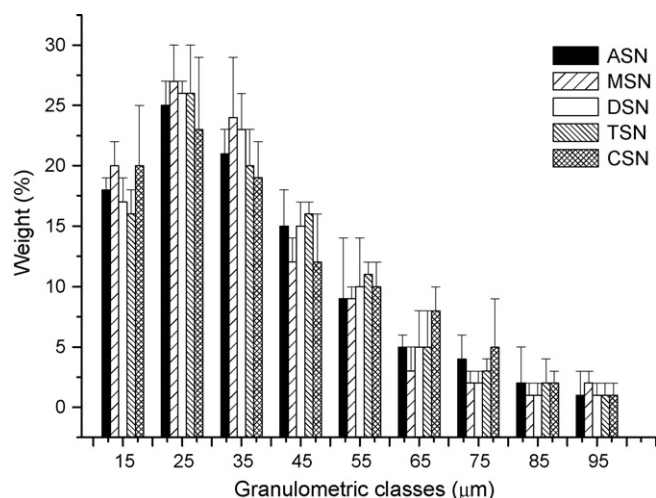


Fig. 2. Particle size and distribution of sodium naproxen particles. ASN: anhydrous sodium naproxen; MSN: monohydrated sodium naproxen; DSN: dihydrated sodium naproxen; TSN: tetrahydrated sodium naproxen; CSN: crystallized sodium naproxen.

frequently proved to be an exception to that observed for the other samples.

The degree of hydration also showed clear repercussions on bulk and tapped densities: they ranked in the order $CSN < ASN < MSN < DSN < TSN$; therefore, bulk and tapped densities significantly increased with increasing hydration degree. Again, the only exception occurred with CSN, which had the lowest densities. The Carr's index, which indicates the ability of a powder to reduce in volume, as will be explained later, affects particle rearrangement at the initial stage of compression. Particle densities have repercussions on powder flowability, as proven by the Carr's indexes: in this study, the Carr's index decreased, and thus flowability increased, as the hydration degree increased, except, again, for the CSN, which exhibited values similar to those of ASN.

3.3. Determination of mechanical properties

Tabletability, one of the most important mechanical characteristics of a pharmaceutical solid material, describes a powder's effectiveness in yielding tablets of satisfactory tensile strength. In particular, tabletability describes the effectiveness of the applied pressure in increasing the tensile strength of the tablet and demonstrates the relationship between the cause, the compaction pressure, and the effect, the strength of the compact (Sun and Grant, 2001a). It has been defined as the capacity of a powder material to be transformed into a tablet of specified strength under the effect of compaction pressure (Joiris et al., 1998).

The tabletability of SN samples is reported in Fig. 3a and followed the order $TSN > CSN \gg DSN > MSN \gg ASN$. The tabletability of TSN was always the highest, though at higher compaction pressures (over 170 MPa), the tabletabilities of TSN and CSN came closer. In fact, the tabletability curves of these two compounds appeared quite linear in the range 20–120 MPa, where the tablet tensile strength proportionally increased with the compression pressure, but over this pressure the TSN curve gradually levelled off, while that of CSN continued to increase slightly.

By taking into account only ASN, MSN, DSN and TSN powders, the tabletability results clearly suggest that the presence of water in the crystalline structure enhances tabletability, and that this enhancement increases as the water content in the lattice increases. This result is in agreement with a previous study (Joiris et al., 2008) demonstrating that the tablet tensile strength increased as the SN water content increased during its hydration. If hydration were

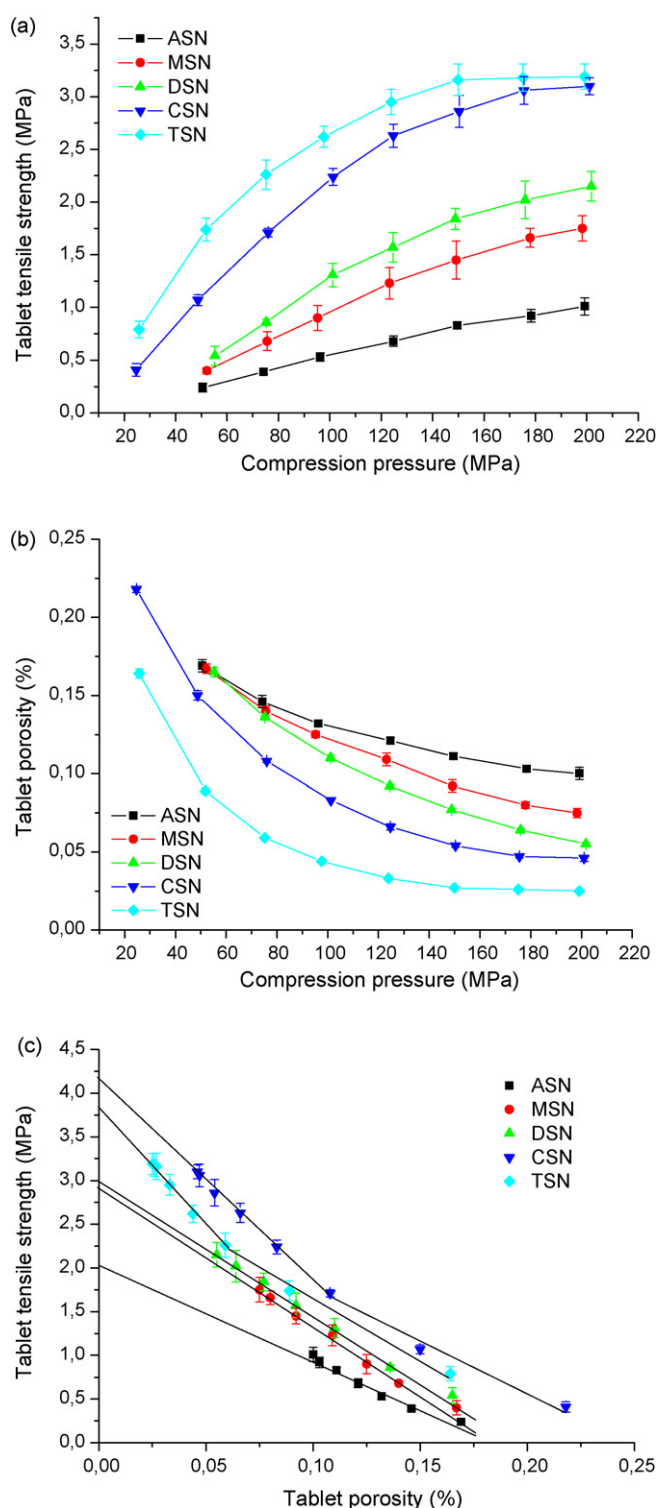


Fig. 3. (a)–(c) Tabletability, compressibility and compactibility of SN powders. Each point is representative of five acquisitions and 95% confidence intervals are indicated as error bars.

the only parameter affecting tabletability, one might expect the tabletability behaviour of DSN and CSN to be similar, because they have the same hydration degree. However, CSN tabletability was considerably higher than that of DSN, and even approached that of TSN at higher compression pressures, as mentioned earlier. Since, as previously proven, the particle morphology and size of these two forms, as well as their total water content, are very close, and

since small differences cannot explain the substantial difference in tabletability, there must be other factors involved in this behaviour; further considerations follow in Section 4. Tabletability describes the relationship between compaction pressure and tablet strength, but does not provide a fundamental understanding of the relationship. Therefore, tabletability alone does not adequately describe tabletability performance (Sun and Grant, 2001a).

In fact, the ability of a powder to give tablets of satisfactory tensile strength can be related either to the number of bonds (the bonding area) (compressibility) or to the strength of these bonds (compactibility).

Compressibility is the ability of a material to undergo a reduction in volume as a result of an applied pressure (Joiris et al., 1998). Thus, compressibility indicates the ease with which a powder bed undergoes volume reduction under compaction pressure and is represented by a plot showing the reduction of tablet porosity with increasing compaction pressure (Sun and Grant, 2001a) (Fig. 3b). At the lowest compression pressure, the tablet porosities of ASN, MSN and DSN were the same. This means that at the highest porosity, the small differences in tabletability cannot depend on the interparticulate bonding area. In addition, TSN also exhibited this same maximum porosity at lower compression pressures. Thus one can rule out the idea that differences in tabletability are due to the interparticulate bonding area. It is also significant that at the same minimal compression pressure, TSN exhibited lower tablet porosity than CSN; thus a possible explanation for TSN's better tabletability is that it has a larger interparticulate bonding area than CSN at lower porosities.

When the compression pressure was increased, compressibility data reflected the results observed for tabletability: curves were aligned from ASN to TSN in the same order previously observed for tabletability (TSN > CSN > DSN > MSN > ASN). In addition, when the initial and final porosities were taken into consideration, the total tablet porosity decreased respectively 41, 55, 67, 79 and 85%, in the order ASN, MSN, DSN, CSN and TSN. Again, CSN compressibility differed from that of DSN, confirming that CSN's higher tabletability can be related to its greater tendency to densify when compression pressure is applied, even if porosities tend to be the same at the higher pressures.

It should be noted that at the highest compression pressure, TSN had far lower porosity than CSN, even though at this pressure the tablet tensile strength of these two forms was the same. Thus it is not unreasonable to suppose that the similar tensile strength of TSN and CSN at the higher pressure is due to factors other than compressibility, an idea that will be considered in more detail below. In general, it is possible to state that tabletability is affected by the ability of these materials to undergo a reduction in volume as a result of an applied pressure.

Compactibility refers to the ability of a material to produce tablets with sufficient strength under the effect of densification (Joiris et al., 1998). It shows the tensile strength of a tablet normalized by tablet porosity (Sun and Grant, 2001a) (Fig. 3c). In many cases, the tensile strength of a tablet decreases exponentially with increasing porosity (Ryshkewitch, 1953). In this study, the compactibility of all the samples was described by Ryshkewitch's equation (Ryshkewitch, 1953):

$$\sigma = \sigma_0 e^{-a\varepsilon} \quad (7)$$

where σ is the tensile strength of porous tablets, ε is the porosity, σ_0 is the tensile strength extrapolated to zero porosity, and a is a constant that may be linked to the pore distribution within a tablet. For all the powders, the tensile strength decreased exponentially with increasing porosity.

Several considerations arise from the compactibility study:

- For ASN, the slope of the plot of $\ln(\sigma)$ vs. porosity and the tensile strength extrapolated at zero porosity (σ_0) (Table 2) were the lowest ones, indicating that ASN has the worst ability to reduce in porosity, and hence has the worst tablet strength.
- The slope and the tensile strength extrapolated at zero porosity (σ_0) of MSN and DSN were practically the same, indicating that there is a similar distribution of pores in the tablets (corroborated by similar particle size and shape) and a similar mechanism in reducing tablet porosity as the compression pressure increases.
- The slopes of the plots of the CSN and the TSN changed with the compression pressures, and were similar for the two powders; similar slope change has been previously described by Sun and Grant (2004), who assumed that the change of slope of the monohydrated form of *p*-hydroxybenzoic acid might reflect a change of consolidation mechanism at higher pressures.
In the case of both CSN and TSN, slopes were similar in the higher porosity range (lower compression pressures), indicating similar initial pore distribution, due to similar particle size and shape, as well as similar initial particle rearrangement and deformation. As the porosity decreased (higher compression pressure), the densification mechanism can be modified and probably plastic deformation becomes the most predominant densification mechanism, accompanied by very low elastic properties. The tensile strength extrapolated at zero porosity (σ_0) of the CSN was slightly higher than that of TSN.
- At the same tablet porosity, the CSN always exhibited higher tensile strength than TSN, even though TSN always exhibited better tabletability. Therefore, the higher tabletability of TSN is a result of its greater interparticulate bonding area (compressibility) and not of its greater bonding strength (compactibility); CSN's higher bonding strength and greater interparticulate bonding area can explain its tabletability superior to that of DSN.

In order to better understand the mechanism responsible for porosity reduction, Heckel's analysis can be used to evaluate densification under compression; in the present study, this analysis was carried out by the "in die" method (Sun and Grant, 2001b).

The Heckel's parameters are indicated in Table 3. D'_0 takes into account the densification by particle slippage and rearrangement occurring at the initial stage of compression, when a pre-compression pressure of 3.0 MPa was applied. In the previous study (Joiris et al., 2008), D'_0 increased with increasing hydration degree. In this work, previous results were confirmed in part and D'_0 increased in the order MSN < DSN < TSN < CSN < ASN. Thus, contrary to expectations, ASN and CSN underwent higher densification during this compression stage. Taking into account their lowest bulk densities (Table 2), it is possible that the higher densification is simply due to the lower bulk density of the powders. It is also interesting to note that D'_0 decreased by decreasing hydration degree for TSN, DSN and MSN, results that once more are in accordance with the bulk density.

D'_B takes into account the fragmentation tendency of the particles during the initial stage of compression. D'_B increased in the order CSN < DSN < MSN < ASN < TSN.

In the previous study (Joiris et al., 2008), D'_B decreased as long as the hydration proceeded and, at the end of hydration, the TSN D'_B was the highest.

In this case, it is difficult to discern a relationship between the water amount and the fragmentation ability. Thus, even though ASN has a pronounced propensity to fragment, its new surfaces were unable to form strong and resistant particles bonds: in other words, fragmentation and formation of new surfaces are not enough to create strong bonds. Such a result is not a trivial one, as it

Table 3

Heckel's parameters obtained from a single compression cycle and total elastic recovery. Data are the mean of five acquisitions and 95% coefficient variation is indicated.

| | ASN | MSN | CSN | DSN | TSN |
|---|---------------|---------------|---------------|---------------|---------------|
| D'_0 (at 3.0 MPa) | 0.663 ± 0.003 | 0.602 ± 0.003 | 0.639 ± 0.009 | 0.618 ± 0.004 | 0.631 ± 0.009 |
| D_A | 0.814 ± 0.001 | 0.728 ± 0.002 | 0.747 ± 0.001 | 0.733 ± 0.001 | 0.794 ± 0.003 |
| $D'_B (D_A - D'_0)$ | 0.151 ± 0.002 | 0.126 ± 0.01 | 0.108 ± 0.010 | 0.114 ± 0.004 | 0.163 ± 0.004 |
| P_Y (MPa) | 124.5 ± 1.4 | 99.8 ± 2.4 | 85.3 ± 0.3 | 97.3 ± 0.8 | 59.0 ± 2.2 |
| Total elastic recovery (%) ^a | 6.95 ± 0.42 | 4.07 ± 0.28 | 3.00 ± 0.16 | 3.07 ± 0.05 | 1.50 ± 0.13 |

^a Total elastic recovery

$$\text{TER} = \frac{t_2 - t_1}{t_1} \times 100$$

t_1 : minimal tablet thickness, when the maximum pressure is applied (150 MPa); t_2 : tablet thickness.

is often found that smaller particles lead to harder tablets (Eriksson and Alderborn, 1995; Di Martino et al., 2000).

The mean yield pressure decreased in the order ASN > MSN > DSN > CSN > TSN. Thus, in general, it is possible to conclude that the plastic deformation increased with increasing hydration. In addition, CSN showed higher plasticity than DSN, so it is possible that plasticity is the mechanism behind its better tableability.

The very high plastic deformability of TSN, together with its very low elastic recovery, can explain its excellent tableability. The elastic recovery decreased in the order ASN > MSN > DSN ≈ CSN > TSN. This parameter is in good agreement with the sample tableability and in general, samples characterized by lower tableability also show higher elastic recovery.

4. Discussion

The results of the compression study indicated the importance of the interparticle bonding in improving the tableability of TSN and CSN with the respect of the anhydrous form and the other hydrated forms. In particular, an increase in the interparticulate bonding area favoured by the high plastic deformability as well by the low elastic recovery of TSN and CSN may explain their compression behaviour. In addition, a certain higher strength of interparticulate bonds may explain the good compression behaviour of the CSN, particularly with the respect to the DSN. At this point, it is necessary to found the explanation of the compression and densification behaviours at a crystalline level. According to Morris (1999), the SN forms obtained by a hydration process can be classified as “channel hydrates”. Di Martino et al. (2008) suggested that during hydration, water molecules move preferentially from the periphery of the crystals along hydrophilic tunnels in the crystal structure that correspond to the propionate side chain. For example, in the case of DSN, two water molecules could easily be accommodated between the SN molecules by forming hydrogen bonds with both Na and/or O atoms. Hydration, which is responsible for a progressive increase in mechanical performance from anhydrous form to monohydrate, dihydrate and tetrahydrate forms, is responsible for crystal expansion, a phenomenon that has been well described by Morris (1999), who referred to “expanded channel hydrates”. In this case, water molecules are mainly bound together by hydrogen bonds and interact little with the host molecule. The presence of water weakens the strength of bonds between adjacent crystalline planes, which consequently behave like sliding planes under compression. This may explain the modifications in compression behaviour of crystals and their tendency to densify under compression pressure.

Interestingly, a typical characteristic of “expanded channel hydrates” is an easy and progressive hydration of crystals under the effect of relative humidity. In the case of SN, this hydration is responsible for the proportional inclusion of water molecules from MSN, DSN to TSN. Thus, a greater number of water molecules may be accommodated in the intermolecular spaces; the progressive

inclusion of water molecules in these spaces increases the distance between some crystalline planes, in proportion to the amount of water. The dimension of the planes depend on the number of water molecules placed in the expanded channel (one for the monohydrate, two for the dihydrate and four for the tetrahydrate). This behaviour is responsible for the progressive increase in plastic deformation of hydrated forms, since the presence of water layers weakens the crystallographic structure, favouring the sliding of adjacent planes. This phenomenon is proportional to the increase in water content inside the crystal, as well as the modification of the densification mechanism from fragmenting to plastic deformation.

TSN possesses the best compression behaviour because the channels are highly expanded by the presence of a greater number of water molecules, which markedly weaken the strength of the bonds between adjacent planes (because the number of water molecules is higher and planes are more distant).

CSN, instead, behaves quite differently under compression, particularly compared to DSN, which has the same content of water molecules. Malaj et al. (2009) showed that the arrangement of water in CSN crystals is completely different from that of DSN obtained by a hydration process. In the case of CSN, the lattice is formed by dissolving and crystallizing SN from water and thus by nucleation and progressive crystal growth. Water molecules are progressively included in the crystal structure, as long as the crystal growth occurs (Malaj, 2009). On the contrary, in the case of DSN, during the hydration process, water molecule access into the crystal is limited by some hydrophobic sites, mainly formed by the π cloud of the naphthalene rings. The water molecules thus move preferentially along hydrophilic tunnels in the crystal structure and corresponding to the propionate side chain; they can be easily accommodated between the SN molecules by forming hydrogen bonds with both Na and/or O atoms (Joiris et al., 2008).

This assumption has been confirmed by dehydration studies demonstrating that, in the case of CSN, water must move through defects in the crystals or sites previously occupied by water molecules, while in the case of DSN, water can move more easily through the same channels through which it gained access during hydration (Malaj et al., 2009). This may account for the different compression and densification behaviour. Even if CSN structure cannot be characterized by the presence of sliding planes, water molecules inserted in the SN crystalline structure do weaken the lattice. The presence of water molecules in the CSN lessen the strength of bonds between adjacent SN molecules. The structure becomes more deformable and the mechanism of compression (plasticity) depends on this tendency.

It is well known the important role of water as binder between particles, effect that in this study was deliberately levelled off since the objective was to evaluate how the water bound in the SN crystalline structure influences compression behaviour, separately from the effect exhibited by the water absorbed on the particle surface. Anyway, it may also be possible to consider that water included in the “expanded channels” since it is not stoichiometrically included in the crystal may act as binder between new particle

surfaces formed during compression, as long as the interparticulate bonding area increases.

5. Conclusion

Though a correlation between SN water content and mechanical properties has already been established by studies considering different experimental approaches (Di Martino et al., 2008; Joiris et al., 2008), the present work has finally made it possible to draw conclusions about the role of water in influencing the behaviour under compression of SN in its anhydrous and hydrate forms, independently of other technological characteristics. The sites in which water molecules are accommodated in the crystalline structure behave like weak points where the crystalline structure may yield under the application of compression pressure. This can lead to deformation and densification of the SN crystalline structure, and particles may come in contact, establishing new interactions. The number and the strength of these interactions are fundamental, but they must be evaluated together with the possibility of irreversible and durable deformation (high plastic deformation and low elastic recovery).

Acknowledgement

The authors would like to thank Sheila Beatty for her linguistic revision of this text.

References

- Armstrong, N.A., Haines-Nutt, R.F., 1974. Elastic recovery and surface area changes in compacted powder systems. *Powder Technol.* 9, 287–290.
- Carr, R.L., 1965a. Evaluating flow properties of solids. *Chem. Eng.* 72, 163–168.
- Carr, R.L., 1965b. Classifying flow properties of solids. *Chem. Eng.* 72, 69–72.
- Di Martino, P., Di Cristofaro, R., Barthélémy, C., Joiris, E., Palmieri, G.F., Martelli, S., 2000. Improved compression properties of propyphenazone spherical crystals. *Int. J. Pharm.* 197, 95–106.
- Di Martino, P., Barthélémy, C., Palmieri, G.F., Martelli, S., 2001. Physical characterization of naproxen sodium hydrate and anhydrate forms. *Eur. J. Pharm. Sci.* 14, 293–300.
- Di Martino, P., Barthélémy, C., Joiris, E., Capsoni, D., Masic, A., Massarotti, V., Gobetto, R., Martelli, S., Bini, M., 2007. A new tetrahydrated form of sodium naproxen. *J. Pharm. Sci.* 96, 156–167.
- Di Martino, P., Malaj, L., Censi, R., Martelli, S., 2008. Physico-chemical and technological properties of sodium naproxen granules prepared in a high-shear mixer–granulator. *J. Pharm. Sci.* 97, 5263–5273.
- Doelker, E., 1994. Assessment of powder compaction. In: Chulia, D., Deleuil, M., Pourcelot, Y. (Eds.), *Powder Technology and Pharmaceutical Process*. Elsevier, Amsterdam, pp. 403–471.
- Eriksson, M., Alderborn, G., 1995. The effect of original particle size and tablet porosity on the increase in tensile strength during storage of sodium chloride tablets in a dry atmosphere. *Int. J. Pharm.* 113, 199–207.
- Fell, J.T., Newton, J.M., 1970. Determination of tablet strength by the diametral-compression test. *J. Pharm. Sci.* 5, 688–691.
- Heckel, R.W., 1961. Density–pressure relationships in powder compaction. *Trans. Metall. Soc. AIME* 221, 661–675.
- Joiris, E., Di Martino, P., Berneron, C., Guyot-Hermann, A.-M., Guyot, J.C., 1998. Compression behaviour of orthorhombic paracetamol. *Pharm. Res.* 15, 1122–1130.
- Joiris, E., Di Martino, P., Malaj, L., Censi, R., Barthélémy, C., Odou, P., 2008. Influence of crystal hydration on the mechanical properties of sodium naproxen. *Eur. J. Pharm. Biopharm.* 70, 345–356.
- Justi, M.J., Paronen, T.P., 1980. On the accuracy of displacement measurements by instrumented single-punch machine. *J. Pharm. Pharmacol.* 32, 796–798.
- Kim, Y., Rousseau, R.W., 2004. Characterization and solid-state transformations of the pseudopolymorphic forms of sodium naproxen. *Cryst. Growth Des.* 4, 1211–1216.
- Khankari, R.K., Grant, D.J.W., 1995. Pharmaceutical hydrates. *Thermochim. Acta* 248, 61–79.
- Kontny, M.J., Zografi, G., 1995. Sorption of water by solids. In: Brittain, H.G. (Ed.), *Physical Characterization of Pharmaceutical Solids*. Marcel Dekker, New York, pp. 387–418.
- Malaj, L., Censi, R., Di Martino, P., 2009. Dehydration of hydrated forms of sodium naproxen. *Cryst. Growth Des.* 9, 2128–2136.
- Malamataris, S., Goidas, P., Dimitriou, A., 1991. Moisture sorption and tensile strength of some tableted direct compression excipients. *Int. J. Pharm.* 68, 51–60.
- Morris, K.R., 1999. Structural aspects of hydrates and solvates. In: Brittain, H.G. (Ed.), *Polymorphism in Pharmaceutical Solids*. Marcel Dekker, New York, pp. 125–181.
- Paronen, P., Ilkka, J., 1996. Porosity–pressure functions. In: Alderborn, G., Nyström, C. (Eds.), *Pharmaceutical Powder Compaction Technology*. Marcel Dekker, New York, pp. 55–75.
- Ryshkewitch, E., 1953. Compression strength of porous sintered alumina and zirconia. *J. Am. Ceram. Soc.* 36, 65–68.
- Sun, C., Grant, D.J.W., 2001a. Influence of crystal structure on the tableting properties of sulfamerazine polymorphs. *Pharm. Res.* 18, 274–280.
- Sun, C., Grant, D.J.W., 2001b. Influence of elastic deformation of particles on Heckel analysis. *Pharm. Dev. Technol.* 6, 193–200.
- Sun, C., Grant, D.J.W., 2004. Improved tableting properties of p-hydroxybenzoic acid by water of crystallization: a molecular insight. *Pharm. Res.* 21, 382–386.